具有金属–金属作用单核自组装体的合成
及其对 Suzuki 偶联反应的高效催化

胡志勇[1]　邓　威[1]　路红琳[1]　黄海平[*,2]　于澍燕[*,1]

([1] 北京工业大学环境与能源工程学院,绿色催化与分离北京市重点实验室,

自组装化学实验室,北京　100124)

([2] 天津民祥生物医药股份有限公司,天津　300350)

摘要: 以配体二苯乙酰丙酮(L)与金属组装子[(bpy)Pd(NO$_3$)]NO$_3$、[(bpy)Pt(NO$_3$)]NO$_3$ 和[(phen)Pd(NO$_3$)]NO$_3$ 在溶液中通过自组装配位作用,自发去质子形成了一系列单核组装体[(bpy)Pd(L)]NO$_3$ (**1**·NO$_3$·H$_2$O)、[(bpy)Pt(L)]NO$_3$ (**2**·NO$_3$·H$_2$O)和[(phen)Pd(L)]NO$_3$ (**3**·NO$_3$·H$_2$O)(其中,bpy=2,2′-联吡啶,phen=1,10-菲咯啉)。这些组装体在含有 KPF$_6$ 的水溶液中能够有效的将 NO$_3^-$ 置换成 PF$_6^-$。NMR 和 ESI-MS 分析确定了这 3 个组装体的单核结构。**1**·PF$_6$·CH$_3$CN 化合物的单晶 X 射线衍射分析表明分子间 π-π 堆积作用与弱的 Pd···Pd 键(0.322 4 nm)相互作用使化合物形成二聚体结构。更为重要的是,这些组装体可作为新颖、高效的 Suzuki 偶联反应催化剂。

Mononuclear Assemblies with Metal-Metal Interaction:
Syntheses and Catalytical Performance in Suzuki-Coupling Reaction

HU Zhi-Yong[1]　　DENG Wei[1]　　LU Hong-Lin[1]　　HUANG Hai-Ping[*,2]　　YU Shu-Yan[*,1]

([1]*Beijing Key Laboratory for Green Catalysis and Separation, Laboratory for Self-Assembly Chemistry, Department of Chemistry and Chemical Industry, College of Environmental and Energy Engineering, Beijing University of Technology, Beijing 100124, China*)
([2]*Tianjin Minxiang Biomedical Co., Ltd., Tianjin 300350, China*)

Abstract: A series of mononuclear complexes named [(bpy)Pd(L)]NO$_3$ (**1**·NO$_3$·H$_2$O), [(bpy)Pt(L)]NO$_3$ (**2**·NO$_3$·H$_2$O), and [(phen)Pd(L)]NO$_3$ (**3**·NO$_3$·H$_2$O) (where bpy=2,2′-bipyridine, phen=1,10-phenanthroline) have been self-assembled through a directed coordination approach that involves spontaneous deprotonation of the 1,3-diphenylpropane-1,3-dione (L) in aqueous solution driven by coordination effect. NO$_3^-$ in these assemblies can be effectively replaced by PF$_6^-$ in a solution of KPF$_6$. All of these new mononuclear complexes have been fully characterized by ^{1}H NMR, ^{13}C NMR and ESI-MS analysis. X-ray diffraction analysis of **1**·PF$_6$·CH$_3$CN clearly shows that a dimeric crystal structure is formed by the π-π stacking interactions and weak intramolecular Pd···Pd (0.322 4 nm) interactions. More importantly, all of these three assemblies can be employed as a new kind of high-efficiency catalysts for Suzuki-coupling reaction. CCDC: 1566337, **1**·PF$_6$·CH$_3$CN.

Spontaneous and precise assembly of compounds into giant, well-defined, functional superstructures are attractive for their novel structures[1-4] and promising applications in molecular recognition, catalysis, guest inclusion, luminescence, anion complexation and so on[5-9]. Over the last decade, numerous novel metal-organic molecules have been constructed by metal-directed self-assembly[10-14]. The Fujita group has established a series of complexes that can be self-assembled by simply mixing ligands and bare square-planar Pd(Ⅱ) ions[15-16]. And in our previous research, we have reported an array of well-defined metallic supramolecular structures formed by quantitatively assembling[17-18]. More recently, transition metals with specific coordination geometries have been employed for the rational design and construction of highly ordered supramolecular structures[19].

Owing to the fact that the aryl-aryl structure motif is an important building block in organic chemistry, the Suzuki reaction is widely applied in academic research as well as in industrial synthesis of fine chemicals and highly complex pharmaceuticals[20]. A representative Suzuki-Miyaura cross-coupling reaction is shown in Scheme 1. In the Suzuki reaction, Pd-based catalysts coordinated with organophosphorus ligands are frequently used in Suzuki-crossing reactions. Since the organophosphorus ligands are
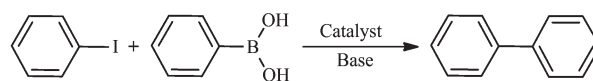
Scheme 1　Representative Suzuki-Miyaura cross-coupling reaction

poisonous, from the environmental point of view, making the Suzuki reaction green is a continuous process pursued by organic chemists. In the past few years, considerable attention has been paid to functional metal-organic assemblies that show promise in catalysis with environment-friendly[21]. Especially, palladium and platinum were employed in the Suzuki coupling reactions for their high stability and remarkable efficiency[22].

In this work, we designed and synthesized three mononuclear complexes using the self-assembly approach, namely [(bpy)Pd(L)]NO$_3$ (**1**·NO$_3$·H$_2$O), [(bpy)Pt (L)]NO$_3$ (**2**·NO$_3$·H$_2$O), and [(phen)Pd(L)]NO$_3$ (**3**·NO$_3$· H$_2$O), respectively. All of these three complexes have been intensively studied by NMR and ESI-MS, and X-ray single-crystal diffraction analysis have been employed for complex **1**·PF$_6$·CH$_3$CN. In addition, considering the structural characteristics and the palladium and platinum （Ⅱ，Ⅱ）properties, these three well-defined complexes have been developed and applied into Suzuki-coupling reactions, as expected, all of these three complexes show excellent catalysis properties.
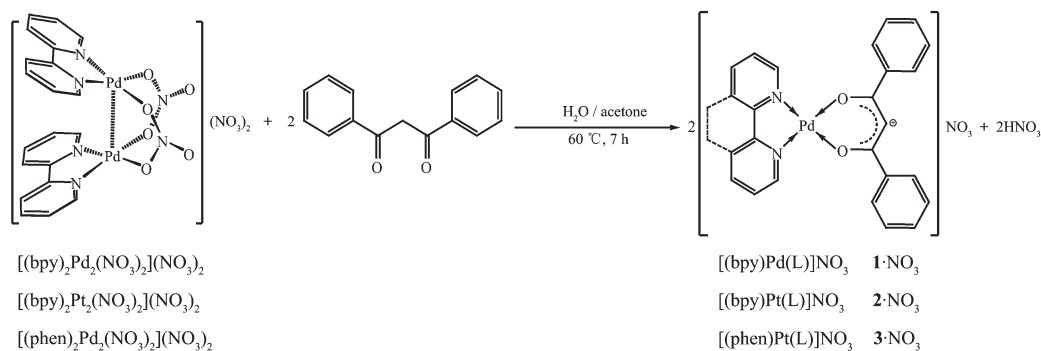
Scheme 2　Self-assembly of complexes **1**·NO$_3$·H$_2$O, **2**·NO$_3$·H$_2$O and **3**·NO$_3$·H$_2$O

1　Experimental

1.1　Materials and instruments

All chemicals for synthesis and analysis were obtained commercially with analytical grade and used without further purification. All solvents were of reagent pure grade and were purified according to conventional methods.

The ESI-MS were performed on a JEOL Accu-TOF mass spectrometer. ^{1}H and ^{13}C NMR spectra were

performed on a Bruker AV 400 MHz spectrometer.

1.2 Syntheses and characterization of mononuclear complexes[23]

The self-assembly of mononuclear Pd complex $1 \cdot$ $NO_3 \cdot H_2O$ was shown in Scheme 2. Ligand L (11.2 mg, 0.05 mmol) was treated with $[(bpy)_2Pd_2(NO_3)_2](NO_3)_2$ (19.3 mg, 0.025 mmol) in a mixture of water and acetone with 2:1 molar ratio. The mixture was stirred at 60 ℃ for 7 h to give $1 \cdot NO_3 \cdot H_2O$. ^1H NMR of $1 \cdot$ $NO_3 \cdot H_2O$ (400 MHz, DMSO-d_6, 298 K, TMS)：δ 8.27 (m, J=7.9 Hz, 4H), 8.11 (t, J=7.7 Hz, 2H), 7.83 (d, J= 7.5 Hz, 4H), 7.61 (m, J=7.4 Hz, 4H), 7.39 (t, J=7.8 Hz, 4H), 6.76 (s, 1H). ^{13}C NMR for $1 \cdot NO_3 \cdot H_2O$ (400 MHz, DMSO-d_6, 298 K, TMS): δ 181.32, 155.96, 147.28, 142.56, 135.15, 133.30, 129.30, 128.48, 124.62, 96.84, 49.07. ESI-MS (CH$_3$CN, m/z): Calcd. for $[(bpy)Pd(L)]^+$ 485.05, Found 485.01. Elemental analysis calculated for $1 \cdot NO_3 \cdot H_2O$ (C$_{25}$H$_{21}$N$_3$O$_6$Pd, %): C: 53.06, H: 3.74, N: 7.43. Found(%): C: 53.03, H: 3.76, N: 7.42. A ten-fold excess of KPF$_6$ was added to the solution, the yellow precipitation were collected by centrifugation, washed with minimum amount of water and dried in vacuum to give $1 \cdot PF_6 \cdot H_2O$ as pale yellow solid (32.1 mg, 0.049 mmol, 97% yield). Single crystals of $1 \cdot PF_6 \cdot$ CH$_3$CN were obtained by the slow vapor diffusion of diethyl ether into their acetonitrile solutions over two weeks. The needle-shaped pale yellow crystals were collected by filtration, washed with water several times and dried in vacuum. ^1H NMR of $1 \cdot PF_6 \cdot H_2O$ (400 MHz, DMSO-d_6, 298 K, TMS): δ 8.38 (d, J=7.8 Hz, 2H), 8.35 (d, J=7.8 Hz, 2H), 8.19 (t, J=7.8 Hz, 2H), 7.93 (d, J= 7.4 Hz, 4H), 7.70 (t, J=6.6 Hz, 2H), 7.62 (t, J=7.3 Hz, 2H), 7.43 (t, J=7.8 Hz, 4H), 6.86 (s, 1H). ^{13}C NMR for $1 \cdot PF_6$ (400 MHz, DMSO-d_6, 298 K, TMS): δ 181.14, 155.83, 147.13, 142.48, 134.98, 133.28, 129.24, 128.41, 124.57, 96.70, 31.15. ESI-MS (CH$_3$CN, m/z): Calcd. for $[(bpy)Pd(L)]^+$ 485.05, Found 485.03. Elemental analysis calculated for $1 \cdot PF_6 \cdot H_2O$ (C$_{25}$H$_{21}$F$_6$N$_2$O$_3$PPd, %): C: 46.28, H: 3.26, N: 4.32. Found(%): C: 46.30, H: 3.30, N: 4.29. Elemental analysis calculated for $1 \cdot PF_6 \cdot$ CH$_3$CN (C$_{27}$H$_{22}$F$_6$N$_3$O$_2$PPd, %): C: 48.27, H: 3.30, N: 6.25. Found(%): C: 48.25, H: 3.32, N: 6.23.

Ligand L (11.2 mg, 0.05 mmol) was treated with $[(bpy)_2Pt_2(NO_3)_2](NO_3)_2$ (23.7 mg, 0.025 mmol) in a mixture of water and acetone with 2:1 molar ratio at 60 ℃ for 7 h to give $2 \cdot NO_3 \cdot H_2O$. ^1H NMR of $2 \cdot NO_3 \cdot$ H_2O (400 MHz, DMSO-d_6, 298 K, TMS): δ 8.64 (d, J= 5.5 Hz, 2H), 8.42 (d, J=8.0, 2H), 8.24 (t, J=7.8 Hz, 2H), 8.03 (d, J=7.8 Hz, 4H), 7.73 (m, J=7.4 Hz, 4H), 7.49 (t, J=7.8 Hz, 4H), 6.94 (s, 1H). ^{13}C NMR (400 MHz, DMSO-d_6, 298 K, TMS): δ 178.37, 156.39, 146.50, 141.87, 134.79, 133.25, 129.39, 128.11, 124.78, 97.32, 49.07. ESI-MS (CH$_3$CN, m/z): Calcd. for $[[(bpy)Pt(L)]]^+$ 574.11, Found 574.07. Elemental analysis calculated for $2 \cdot NO_3 \cdot H_2O$ (C$_{25}$H$_{21}$N$_3$O$_6$Pt, %): C: 45.87, H: 3.23, N: 6.42. Found(%): C: 45.85, H: 3.26, N: 6.40. A ten-fold excess of KPF$_6$ was added to the above solution, the yellow precipitation were collected by centrifugation, washed with minimum amount of water and dried in vacuum to give $2 \cdot PF_6 \cdot H_2O$ as yellow solid (35.6 mg, 0.048 mmol, 95% yield). ^1H NMR confirmed the quantitative formation of $2 \cdot PF_6 \cdot H_2O$. ^1H NMR (400 MHz, DMSO-d_6, 298 K, TMS): δ 8.63 (d, J=5 Hz, 2H), 8.41 (d, J=7.8 Hz, 2H), 8.23 (t, J=7.8 Hz, 2H), 8.02 (d, J=7.4 Hz, 4H), 7.72 (m, 4H), 7.48 (t, J=7.9 Hz, 4H), 6.93 (s, 1H). ^{13}C NMR (400 MHz, DMSO-d_6, 298 K, TMS): δ 178.80, 156.66, 146.77, 142.06, 135.10, 133.29, 129.47, 128.32, 128.21, 124.87, 97.67. ESI-MS (CH$_3$CN, m/z): Calcd. for $[(bpy)Pt(L)]^+$ 574.11, Found 574.09. Elemental analysis calculated for $2 \cdot PF_6 \cdot H_2O$ (C$_{25}$H$_{21}$F$_6$ N$_2$O$_3$PPt, %): C: 40.71, H: 2.87, N: 3.80. Found: C: 40.69, H: 2.88, N: 3.78.

Ligand L (11.2 mg, 0.05 mmol) was treated with $[(phen)_2Pd_2(NO_3)_2](NO_3)_2$ (20.5 mg, 0.025 mmol) in a mixture of water and acetone with 2:1 molar ratio at 60 ℃ for 7 h to give $3 \cdot NO_3 \cdot H_2O$. ^1H NMR of $3 \cdot NO_3 \cdot$ H_2O: (400 MHz, DMSO-d_6, 298 K, TMS): δ 8.93 (d, J= 8.2 Hz, 2H), 8.87 (d, J=5.2 Hz, 2H), 8.23 (s, 2H), 8.15 (m, J=4.7 Hz, 6H), 7.69 (t, J=7.3 Hz, 2H), 7.55 (t, J= 7.6 Hz, 4H), 7.02 (s, 4H). ^{13}C NMR (400 MHz, DMSO-d_6, 298 K, TMS): δ 180.27, 147.95, 145.69, 140.94, 134.31, 133.23, 130.46, 129.09, 128.33, 126.65, 49.07. ESI-MS (CH$_3$CN, m/z): Calcd. for $[(phen)Pd(L)]^+$ 509.05, Found 509.01. Elemental analysis calculated for $3 \cdot$ $NO_3 \cdot H_2O$ (C$_{27}$H$_{21}$N$_3$O$_6$Pt, %): C: 54.97, H: 3.59, N: 7.12. Found(%): C: 55.00, H: 3.56, N: 7.11. A ten-fold

excess of KPF_6 was added to the solution, the yellow precipitation were collected by centrifugation, washed with minimum amount of water and dried in vacuum to give pale yellow solid of $\mathbf{3} \cdot PF_6 \cdot H_2O$. (33.2 mg, 0.049 mmol, 97% yield). ^{1}H NMR confirmed the quantitative formation of $\mathbf{3} \cdot PF_6 \cdot H_2O$. ^{1}H NMR of $\mathbf{3} \cdot PF_6 \cdot H_2O$: (400 MHz, DMSO-$d_6$, 298 K, TMS): δ 8.56 (d, J=8.1 Hz, 2H), 8.48 (d, J=4.4 Hz, 2H), 7.98 (s, 2H), 7.86 (m, 2H), 7.80 (d, J=7.4 Hz, 4H), 7.59 (t, J=7.3 Hz, 2H), 7.37 (t, J=7.8 Hz, 4H), 6.61 (s, 1H). ^{13}C NMR (400 MHz, DMSO-d_6, 298 K, TMS): δ 180.46, 148.01, 145.86, 141.00, 134.46, 133.26, 130.52, 129.13, 128.36, 126.66, 96.02. ESI-MS (CH$_3$CN, m/z): Calcd. for [(phen)Pd(L)][+] 509.05, Found 509.04. Elemental analysis calculated for $\mathbf{3} \cdot PF_6 \cdot H_2O$ ($C_{27}H_{21}F_6N_2O_3PPd$, %): C: 48.20, H: 3.15, N: 4.16. Found: C: 48.18, H: 3.15, N: 4.17.

1.3 X-ray crystallography of complex $\mathbf{1} \cdot PF_6 \cdot CH_3CN$

X-ray diffraction data of the crystals of complex $\mathbf{1} \cdot PF_6 \cdot CH_3CN$ was collected at 150(2) K by using Bruker Smart Apex CCD area detector equipped with a graphite monochromated Mo $K\alpha$ radiation (λ=0.071 073 nm). The structure of $\mathbf{1} \cdot PF_6 \cdot CH_3CN$ was solved by direct method and refined by employing full matrix least-square on F^2 by using SHELXTL (Bruker, 2000) program and expanded using Fourier techniques [24-25]. All non-H atoms of the complex $\mathbf{1} \cdot PF_6 \cdot CH_3CN$ were refined with anisotropic thermal parameters. The hydrogen atoms were included in idealized positions with isotropic displacement parameters constrained to 1.5 times the U_{equiv} of their attached carbon atoms for methylene hydrogens, and 1.2 times the U_{equiv} of their attached carbon atoms for all others. SQUEEZE option was employed to treat the disordered counter anions. The crystallographic data of complex $\mathbf{1} \cdot PF_6 \cdot CH_3CN$ were listed in Table 1 and the selected hydrogen bond lengths and bond angles of complex $\mathbf{1} \cdot PF_6 \cdot CH_3CN$ were listed in Table S1 and S2.

CCDC: 1566337, $\mathbf{1} \cdot PF_6 \cdot CH_3CN$.

Table 1　Crystallographic data for complex $\mathbf{1} \cdot PF_6 \cdot CH_3CN$

Formula	$C_{27}H_{22}F_6N_3O_2PPd$	$F(000)$	1 344
Formula weight	671.84	Index ranges	$-8 \leqslant h \leqslant 8, -21 \leqslant k \leqslant 21, -23 \leqslant l \leqslant 23$
Crystal system triclinic	Monoclinic	θ range / (°)	2.360~25.246
Space group	$P2_1/n$	Reflection collected	12 779
a / nm	0.711 28(6)	Observed reflection with [$I>2\sigma(I)$]	3 521
b / nm	1.807 66(19)	Number of parameter	356
c / nm	1.970 19(15)	Independent reflection	4 436 (R_{int}=0.060 1)
β / (°)	94.296(5)	Goodness-of-fit on F^2	1.096
Volume / nm^3	2.526 1(4)	Final R indices [$I>2\sigma(I)$]	R_1=0.041 1, wR_2=0.100 6
Z	4	R indices (all data)	R_1=0.052, wR_2=0.104 3
D_c / (g·cm^{-3})	1.767	Largest diff. peak and hole / (e·nm^{-3})	1 415 and -1 274
μ / mm^{-1}	0.875		

2　Results and discussion

2.1　Characterization of $\mathbf{1} \cdot PF_6 \cdot H_2O$, $\mathbf{2} \cdot PF_6 \cdot H_2O$ and $\mathbf{3} \cdot PF_6 \cdot H_2O$

NMR were fully carried out to characterize the complexes of $\mathbf{1} \cdot PF_6 \cdot H_2O$, $\mathbf{2} \cdot PF_6 \cdot H_2O$ and $\mathbf{3} \cdot PF_6 \cdot H_2O$. Analysis by ^{1}H NMR spectroscopy of $\mathbf{1} \cdot NO_3 \cdot H_2O$ in DMSO-d_6 solutions clearly showed an array of well-defined resonance and suggested the self-assembly of [(bpy)$_2$Pd$_2$(NO$_3$)$_2$](NO$_3$)$_2$ and L to form a single product (Fig.S1~S2). Upon replaced by PF$_6^-$, a series of peaks shifted downfield as shown in Fig.1. The results of ^{1}H NMR spectroscopy indicated that the formation of a 1:1 complex of $\mathbf{1} \cdot PF_6 \cdot H_2O$. Detailed analysis of ^{1}H NMR spectra belonged to the complex $\mathbf{1} \cdot PF_6 \cdot H_2O$ was discussed as below: for complex $\mathbf{1} \cdot PF_6 \cdot H_2O$, the featured single peak at 6.86 corresponded to methylene-H, the triplet at 7.43 were assigned to aromatic-H2, aromatic-H2′, aromatic-H4 and aromatic-H4′, the triplet at 7.62 with integral of 2 H assigned to pyridine-H7 and
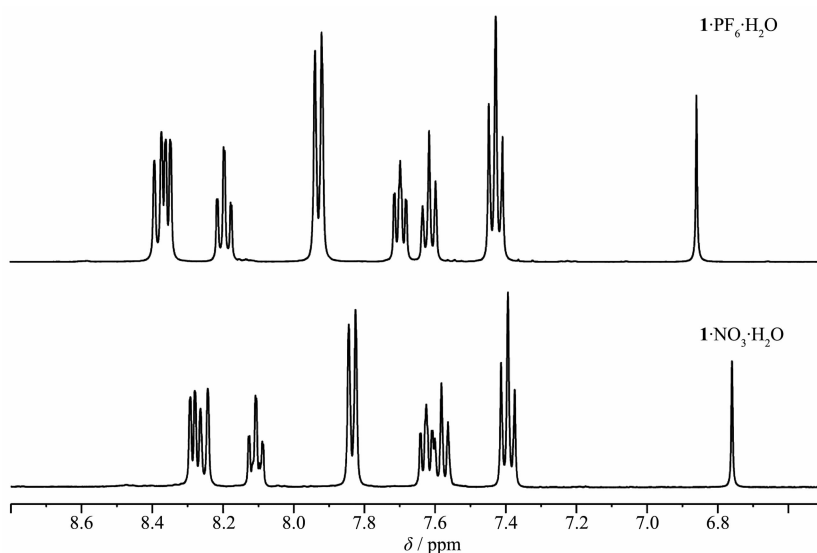
Fig.1　^{1}H NMR spectrum of complex $\mathbf{1}\cdot NO_3\cdot H_2O$ and $\mathbf{1}\cdot PF_6\cdot H_2O$ in DMSO-d$_6$

pyridine-H7′, and the triplet at 7.70 with integral of 2 H assigned to pyridine-H8 and pyridine-H8′, the doublet at 7.93 with integral of 4 H assigned to aromatic -H1, aromatic-H1′, aromatic-H5 and aromatic-H5′, the triplet at 8.19 with integral of 2 H assigned to aromatic-H3 and aromatic-H3′, the downfield 4 H assigned to pyridine-H6, pyridine-H6′, pyridine-H9 and pyridine-H9′, respectively. And the results of ^{13}C NMR spectroscopy as shown in Fig.S8 agreed well with the analysis results of ^{1}H NMR spectroscopy. These results were consistent with those of the complexes $\mathbf{2}\cdot NO_3\cdot H_2O$, $\mathbf{2}\cdot PF_6\cdot H_2O$, $\mathbf{3}\cdot NO_3\cdot H_2O$ and

$\mathbf{3}\cdot PF_6\cdot H_2O$ (Fig.S3~S6 and Fig.S9~S12).

　　ESI-MS studies also confirmed the structure of $\mathbf{1}\cdot NO_3\cdot H_2O$, $\mathbf{1}\cdot PF_6\cdot H_2O$, $\mathbf{2}\cdot NO_3\cdot H_2O$, $\mathbf{2}\cdot PF_6\cdot H_2O$, $\mathbf{3}\cdot NO_3\cdot H_2O$ and $\mathbf{3}\cdot PF_6\cdot H_2O$ in solution (Fig.2, S13~S17). Isotope patterns matched those simulated and peak separations consistent with the charges. When an acetonitrile solution of $\mathbf{1}\cdot PF_6\cdot H_2O$ was subjected to the ESI-MS, prominent peaks for $[(bpy)Pd(L)]^+$ were clearly observed at 485.03, indicating the complete formation of metal-organic complexes. Additionally, the striking peak at 485.03 also confirmed the spontaneous deprotonation of 1,3-diphenylpropane-
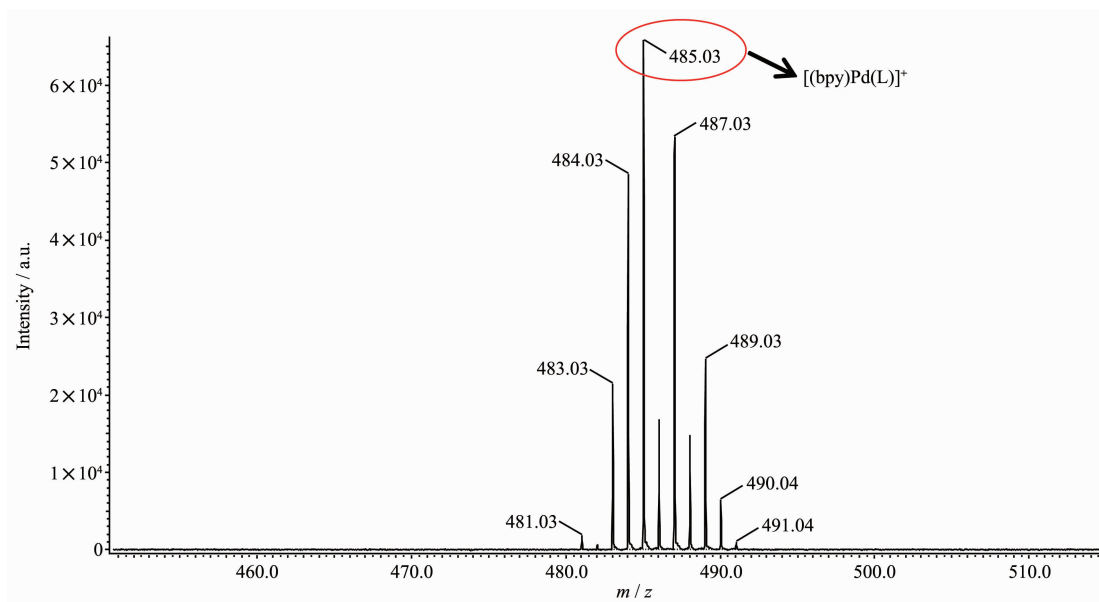
Fig.2　ESI-MS spectrum of complex $\mathbf{1}\cdot PF_6\cdot H_2O$ in acetonitrile

1,3-dione (L) in solution driven by coordination effect. Similarly, the ESI-MS study of $2 \cdot PF_6 \cdot H_2O$ and $3 \cdot PF_6 \cdot H_2O$ afforded a series of peaks at *m/z* 574.09 and 509.04 were similar to that of complex $1 \cdot PF_6 \cdot H_2O$.

2.2 Crystal structure of $1 \cdot PF_6 \cdot CH_3CN$

The molecular structure of complex $1 \cdot PF_6 \cdot CH_3CN$ was unambiguously determined by reliable methods of X-ray diffraction analysis. As shown in Fig.3, complex $1 \cdot PF_6 \cdot CH_3CN$ crystallizes in monoclinic space group $P2_1/n$. The crystal structure of $1 \cdot PF_6 \cdot CH_3CN$ displays a mononuclear palladium(Ⅱ) complex with planar conformation, and a parallel pattern is formed between planes. A dimeric crystal structure is formed by the efficient π-π stacking interactions and the metal-metal interactions, which make the complex of $1 \cdot PF_6 \cdot CH_3CN$ be an efficient catalyst. The central palladium (Ⅱ) is coordinated by two N atoms (the two N atoms of bpy) and two O atoms (the two O atoms of L) in a square

coordination mode. The distances of Pd(1)-O(1) and Pd(1)-O(2) are 0.200 7 and 0.197 8 nm, respectively. And the distances between Pd(1) and the two N atoms are 0.201 6 and 0.198 5 nm, respectively. While the intermolecular Pd(Ⅱ)···Pd(Ⅱ) distance is about 0.322 4 nm, which indicates that the interactions exist between them, and the interaction may be suitable for the catalysis applications of the complex $1 \cdot PF_6 \cdot CH_3CN$. The angles of O(1)-Pd(1)-O(2) and N(1)-Pd(1)-N(2) were 93.06° and 82.10°, respectively. The dihedral angle, defined by planes O(1)-Pd(1)-O(2) and N(1)-Pd(1)-N(2), is 5.48°. Extending *a*, *b* and *c* axes with PF_6^- anions and acetonitrile molecules frozen inside as shown in Fig.3 and S18. The structure determined by X-ray crystallographic analysis agreed well with the NMR and ESI-MS analysis. We had tried many times to obtain the crystals of $2 \cdot PF_6 \cdot CH_3CN$ and $3 \cdot PF_6 \cdot CH_3CN$, but failed.
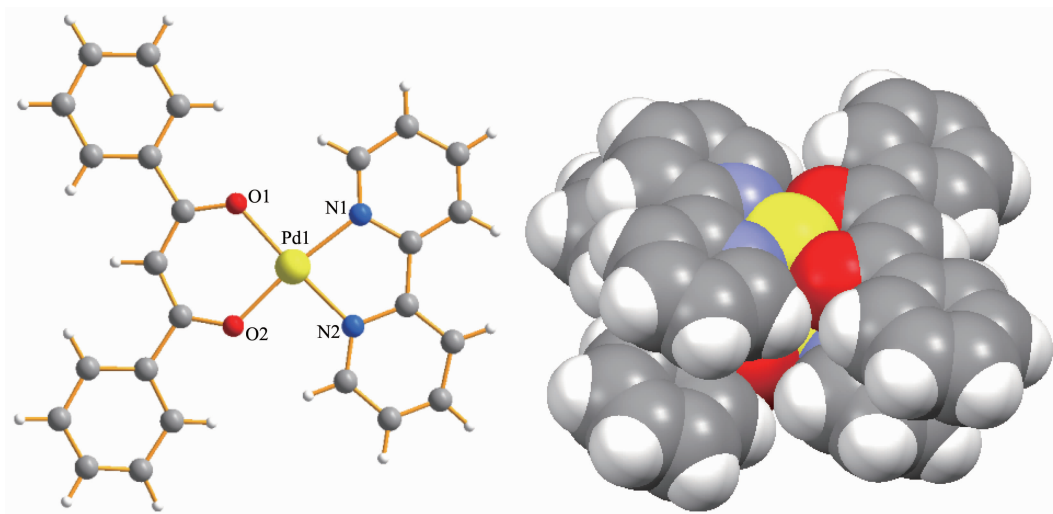
Counter ions and solvent molecules are omitted for clarity

Fig.3　Molecular structure (left) and the dimeric crystal structure (right) of $1 \cdot PF_6 \cdot CH_3CN$

2.3 Catalytic activity

For the importance of the Suzuki cross-coupling reaction and the structural characteristics of palladium and platinum (Ⅱ, Ⅱ) complexes, $1 \cdot PF_6 \cdot H_2O$, $2 \cdot PF_6 \cdot H_2O$ and $3 \cdot PF_6 \cdot H_2O$ were devoted to explore the catalyst activity. In our previous work, we have discussed the catalyst activity of pyrazolate-based dipalladium(Ⅱ) complexes[26]. In this work, different solvents, temperature, reaction time and reagents were examined to optimize the process conditions.

Firstly, effects of different solvents were investigated, and the optimum conditions were shown in Table 2. According to previous experiments records[27], 1,4-dioxane and ethanol were prepared for the catalyst activity, and it was observed that different solvents are suited for different reactions. Meanwhile, the temperature and the reaction time were adjusted to achieve the optimal strategy.

Next, the influence of reagents was explored in the controlled experiments. Different yields but
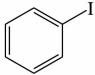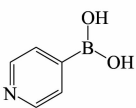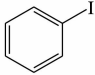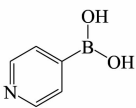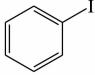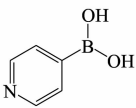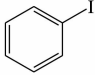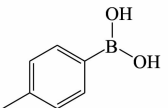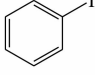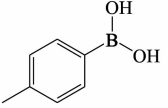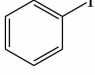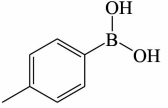
Table 2 Catalytic activity of complexes $1 \cdot PF_6 \cdot H_2O$, $2 \cdot PF_6 \cdot H_2O$ and $3 \cdot PF_6 \cdot H_2O$

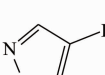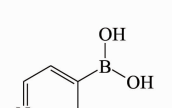| Entry	Catalyst	Co-catalyst	Solvent	T / ℃	Time / h	Yield / %
1	$1 \cdot PF_6 \cdot H_2O$	K_3PO_4	1,4-dioxane	100	12	94
2	$2 \cdot PF_6 \cdot H_2O$	K_3PO_4	1,4-dioxane	100	36	87
3	$3 \cdot PF_6 \cdot H_2O$	K_3PO_4	1,4-dioxane	100	24	89
4	$1 \cdot PF_6 \cdot H_2O$	K_3PO_4	ethanol	80	12	91
5	$2 \cdot PF_6 \cdot H_2O$	K_3PO_4	ethanol	80	24	88
6	$3 \cdot PF_6 \cdot H_2O$	K_3PO_4	ethanol	80	12	92
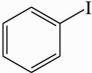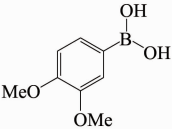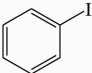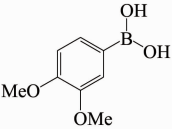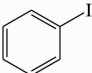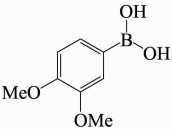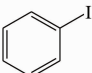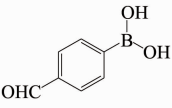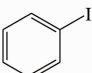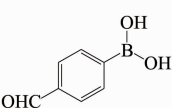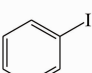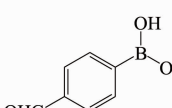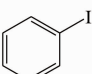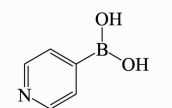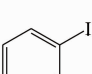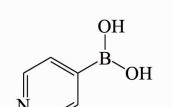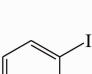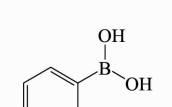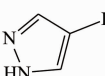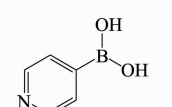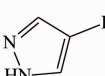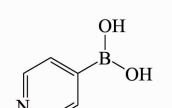
satisfactory results were obtained for the aryl-aryl reactions (Table 3). But for the heterocyclic-based reactions, since the previous set of experiments have consistently use unprotected starting pyrazol-based, the palladium or platinum ions in $1 \cdot PF_6 \cdot H_2O$, $2 \cdot PF_6 \cdot H_2O$ and $3 \cdot PF_6 \cdot H_2O$ complexes could coordinate with the unprotected starting pyrazole, leading to side-products and yield decreasing. Then a series of protected starting pyrazol-based were employed for the cross-coupling reactions, as expected, the yields of

adducts were higher. With the optimized reaction conditions in hand, a broad substrate listed in Table 3 is observed. The results of control experiment and blank experiment show that good catalytic effect would be found only when main catalysts and sub-catalysts coexist simultaneously. It seems that the electronic effect of metal-metal interaction and the steric effect of the catalysts make the reaction efficiency.
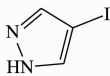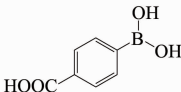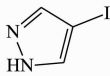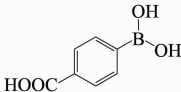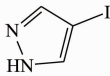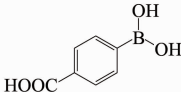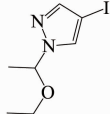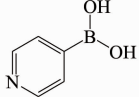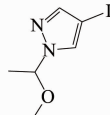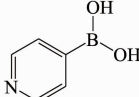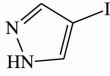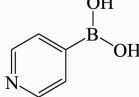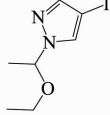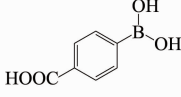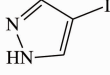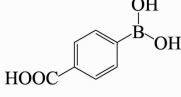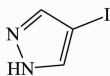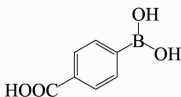
Table 3 Catalytic activity of complexes $1 \cdot PF_6 \cdot H_2O$, $2 \cdot PF_6 \cdot H_2O$ and $3 \cdot PF_6 \cdot H_2O$

Entry	Catalyst	Co-catalyst	Substrate A	Substrate B	Solvent	T / ℃	Yield / %
1	$1 \cdot PF_6 \cdot H_2O$	None			ethanol	100	11.4
2	None	K_3PO_4			ethanol	100	7.3
3	None	None			ethanol	100	7.8
4	$1 \cdot PF_6 \cdot H_2O$	K_3PO_4			1,4-dioxane	100	92
5	$2 \cdot PF_6 \cdot H_2O$	K_3PO_4			ethanol	80	88
6	$3 \cdot PF_6 \cdot H_2O$	K_3PO_4			ethanol	80	89

Continued Table 3

7	**1**·PF$_6$·H$_2$O	K$_3$PO$_4$			1,4-dioxane	100	86
8	**2**·PF$_6$·H$_2$O	K$_3$PO$_4$			ethanol	80	79
9	**3**·PF$_6$·H$_2$O	K$_3$PO$_4$			1,4-dioxane	100	81
10	**1**·PF$_6$·H$_2$O	K$_3$PO$_4$			1,4-dioxane	100	83
11	**2**·PF$_6$·H$_2$O	K$_3$PO$_4$			ethanol	80	73
12	**3**·PF$_6$·H$_2$O	K$_3$PO$_4$			ethanol	80	75
13	**1**·PF$_6$·H$_2$O	K$_3$PO$_4$			1,4-dioxane	100	88
14	**2**·PF$_6$·H$_2$O	K$_3$PO$_4$			ethanol	80	75
15	**3**·PF$_6$·H$_2$O	K$_3$PO$_4$			ethanol	80	82
16	**1**·PF$_6$·H$_2$O	K$_3$PO$_4$			ethanol	80	35
17	**2**·PF$_6$·H$_2$O	K$_3$PO$_4$			ethanol	80	26
18	**3**·PF$_6$·H$_2$O	K$_3$PO$_4$			ethanol	80	29

Continued Table 3

19	$\mathbf{1}\cdot PF_6\cdot H_2O$	K_3PO_4			ethanol	80	25
20	$\mathbf{2}\cdot PF_6\cdot H_2O$	K_3PO_4			ethanol	80	27
21	$\mathbf{3}\cdot PF_6\cdot H_2O$	K_3PO_4			ethanol	80	22
22	$\mathbf{1}\cdot PF_6\cdot H_2O$	K_3PO_4			ethanol	80	72
23	$\mathbf{2}\cdot PF_6\cdot H_2O$	K_3PO_4			ethanol	80	68
24	$\mathbf{3}\cdot PF_6\cdot H_2O$	K_3PO_4			ethanol	80	69
25	$\mathbf{1}\cdot PF_6\cdot H_2O$	K_3PO_4			ethanol	80	67
26	$\mathbf{2}\cdot PF_6\cdot H_2O$	K_3PO_4			ethanol	80	64
27	$\mathbf{3}\cdot PF_6\cdot H_2O$	K_3PO_4			ethanol	80	73

3　Conclusions

In summary, we have synthesized three mono-metallic complexes in quantitative yields by a directed self-assembly of diketone-based ligands with [(bpy)Pd(NO₃)]NO₃, [(bpy)Pt(NO₃)]NO₃ and [(phen)Pd(NO₃)]NO₃ in a 2:1 molar ratio. The assemblies have been chara-cterized by NMR and ESI-MS, and the complex of $\mathbf{1}\cdot PF_6\cdot CH_3CN$ was fully defined by single-crystal X-ray diffraction method. These characterizations show the structural similarity of these assemblies. The single-crystal structures show that weak intramolecular Pd⋯Pd interactions exist in $\mathbf{1}\cdot PF_6\cdot CH_3CN$. More signifi-cantly, these metal-organic species with metal-metal interaction have potential application in the field of Suzuki cross-coupling reaction.

Supporting information is available at http://www.wjhxxb.cn

References:

[1] Frank M, Ahrens J, Bejenke I, et al. *J. Am. Chem. Soc.*, **2016,138**:8279-8287

[2] Klein C, Gütz C, Bogner M, et al. *Angew. Chem., Int. Ed.*, **2014,53**:3739-3742

[3] Luo D, Zhou X P, Li D. *Angew. Chem., Int. Ed.*, **2015,54**: 6190-6195

[4] Yoshizawa M, Yoshizawa Y, Kusukawa T, et al. *Angew. Chem. Int. Ed.*, **2002,41**:1347-1349

[5] Cui Y, Chen Z M, Jiang X F, et al. *Dalton Trans.*, **2017,46**: 5801-5805

[6] Jiang X F, Huang H, Chai Y F, et al. *Nat. Chem.*, **2017,9**: 188-193

[7] Ronson T K, Pilgrim B S, Nitschke J R. *J. Am. Chem. Soc.*, **2016,138**:10417-10420

[8] Liu Y, Kravtsov V, Walsh R D, et al. *Chem. Commun.*, **2004**: 2806-2807

[9] Sun Q F, Liu L X, Huang H P, et al. *Inorg. Chem.*, **2008,47**: 2142-2154

[10]Ward M D, Raithby P R. *Chem. Soc. Rev.*, **2013,42**:1619-1636

[11]Fleming J S, Mann K L V, Carraz C A, et al. *Angew. Chem. Int. Ed.*, **1998,37**:1279-1281

[12]Fiedler D, Leung D H, Bergman R G, et al. *Acc. Chem. Res.*, **2005,38**:349-358

[13]Fujita M, Tominaga M, Hori A, et al. *Acc. Chem. Res.*, **2005, 38**:369-378

[14]Seidel S R, Stang P J. *Acc. Chem. Res.*, **2002,35**:972-983

[15]Tominaga M, Suzuki K, Kawano M, et al. *Angew. Chem. Int. Ed.*, **2004,43**:5621-5625

[16]Suzuki K, Kawano M, Fujita M. *Angew. Chem. Int. Ed.*, **2007,46**:2819-2822

[17]Wang Y Q, Jiang X F, Li H, et al. *Chem. Asian J.*, **2015,10**: 1146-1149

[18]Xie Z T, Guo C, Yu S Y, et al. *Angew. Chem. Int. Ed.*, **2012, 51**:1177-1181

[19]Baxter P N W. *Comprehensive Supramolecular Chemistry*: *Vol.*9. Sauvage J P, Hosseini M W. Ed. New York: Pergamon, **1996**.

[20]Basu B, Biswas K, Kundu S, et al. *Green Chem.*, **2010,12**: 1734-1738

[21]Wang F, Li C, Chen H, et al. *J. Am. Chem. Soc.*, **2013,135**: 5588-5601

[22]Muratsugu S, Maity N, Baba H, et al. *Dalton Trans.*, **2017, 46**:3125-3134

[23]Yu S Y, Fujita M, Yamaguchi K. *J. Chem. Soc. Dalton Trans.*, **2001**:3145-3146

[24]Sheldrick G M. *SHELXS*-97, *Program for the Solution of Crystal Structures*, University of Göttingen, Germany, **1997**.

[25]Sheldrick G M. *SHELXL*-97, *Program for the Refinement of Crystal Structures*, University of Göttingen, Germany, **1997**.

[26]CHEN Han(陈涵), YU Zhi-Chun(于智淳), DENG Wei(邓威), et al. *Chinese J. Inorg. Chem.*(无机化学学报), **2017, 33**:939-946

[27]Hussain N, Borah A, Darabdhara G, et al. *New J. Chem.*, **2015,39**:6631-6641